LESZEK MORAWSKI, Assoc.Prof.,D.Sc.,E.E.
ANDRZEJ RAK, M.Sc.,E.E.
Gdynia Maritime Academy
Department of Ship Automation

Identification of model ship dynamics

SUMMARY

The paper contains identification results of linear, nonlinear and neural models of ship dynamics. Simple SISO and MIMO models were evaluated in their traditional and neural versions. The identification algorithms were effected off-line. The MATLAB numerical software was employed to execute the identification computations. Results of the research completed by using the VLCC tanker model are presented.

INTRODUCTION

One of the methods of defining a ship dynamic model for control systems synthesis purposes is the examination of physical ship models in semi-natural conditions. Such experiments are performed in model basins or open waters. The paper presents results of the research completed by using „Warta" tanker model in the Ship Handling Research and Training Centre in Iława, Poland. The model built in 1:24 scale is shown in Fig.1. General parameters of the model are given in Tab.1.

Tab.1. General model parameters

Length overall	L_{OA}	[m]	12.205
Length between perpendiculars	L_{BP}	[m]	11.583
Breadth	B	[m]	2.000
Draught	H	[m]	0.846
Displacement	D	[t]	12.178
Speed	V_c	[m/s]	1.62
Scale	λ		1:24

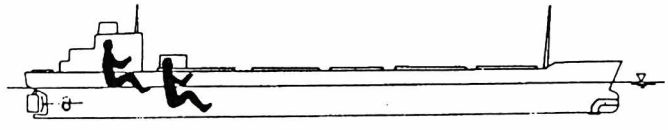

Fig.1. The outline of „Warta" tanker of 145 000 dwt, model in 1:24 scale

The main propulsion , steering gear and bow thruster drives of the model are built with the use of DC motors. Model output power and rotation speed are proportional to its scale. The DC motors are supplied from the high capacity battery sets which permit their continuous running for a few hours. The measurement equipment installed on the model consists of the PC computer connected to the Plath VI gyrocompass, rudder angle converter and, through radio-modem, to a photooptical positioning system [3].

The applied approach to measurements has an advantage of converting their results from a model to full scale directly. On-line inspection of hull behaviour in environmental noises is also possible. This data acquisition and control equipment, except of the photo-optical positioning system, can be applied to full size ships. The paper contains identification results of linear and nonlinear Norrbin's models and neural models of ship dynamics. Simple SISO models which describe relations between the ship heading ψ and the rudder angle δ were elaborated for course keeping system synthesis. Two dimensional models showing relations among the yawing velocity $r=d\psi/dt$, sway velocity v and rudder angle δ were utilized in ship trajectory tracking systems.

GENERAL DESCRIPTION OF SHIP MODEL DYNAMICS

The equations of ship motion on the calm, deep and shallow waters are described by Norrbin [5]. When taking into consideration ship motion on the horizontal plane only, the equations of rolling, pitching and heaving can be substituted by properly modeled disturbances in other equations. To describe ship model motions, two following Cartesian coordinate systems were chosen:

- the earth-fixed X_oY_o system with X_o axis pointed towards the local north direction on the lake, determined by the basement of the photooptical positioning system [3], and

- the hull-fixed, right-handed XYZ coordinate system with X axis pointed forward along the centerline of the ship (Fig. 2).

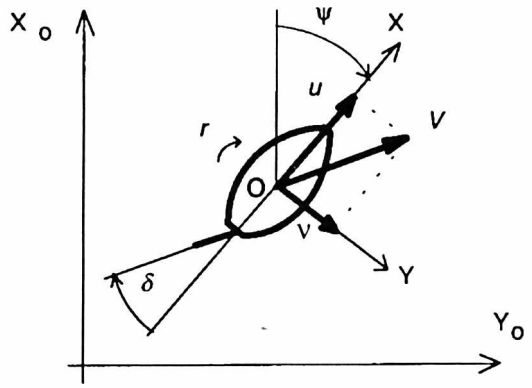

Fig. 2. Cartesian coordinate systems

The hull motion equations on the horizontal plane are derived from the Newtonian mechanics laws applied to forces acting on the hull along X and Y axis and moments relative to Z axis:

$$\begin{aligned} m(\dot{u} - vr - x_G r^2) &= X_S \\ m(\dot{v} + ur + x_G \dot{r}) &= Y_S \\ I_Z \dot{r} + m x_G (\dot{v} + ur) &= N_S \end{aligned} \tag{1}$$

where:

- X_S, Y_S - hydrodynamic forces effecting the hull, acting along X and Y axis, respectively
- N_S - sum of the hydrodynamic moments effecting the hull relative to Z axis
- u, v - longitudinal and transverse components of the velocity vector V, respectively
- m - ship mass
- I_Z - ship moment of inertia relative to Z axis
- x_G - x-coordinate of the ship's centre of gravity, (y_G=0)

The hydrodynamic forces X_S, Y_S and hydrodynamic moment N_S are complex functions of ship motion parameters. Abkowitz proposed their general form as follows [1]:

$$\begin{aligned} X_S &= X_S(u,v,r,\delta,\dot{u},\dot{v},\dot{r}) \\ Y_S &= Y_S(u,v,r,\delta,\dot{u},\dot{v},\dot{r}) \\ N_S &= N_S(u,v,r,\delta,\dot{u},\dot{v},\dot{r}) \end{aligned} \tag{2}$$

LINEAR AND NONLINEAR MODELS

The force and moment functions can be approximated by Taylor expansion about the fix point $u=u_o$, $v=r=\delta=\dot{u}=\dot{v}=\dot{r}=0$. Different mathematical ship motion models can be obtained when omitting different higher-order terms. The linear model is acquired when the Taylor series is bounded to certain first-order terms and adjoined with the kinematic equation which describes changes of the course angle ψ. The model can be expressed in the following manner:

$$\begin{aligned} \dot{v} &= a_{11}v + a_{12}r + b_1\delta \\ \dot{r} &= a_{21}v + a_{22}r + b_2\delta \\ \dot{\psi} &= r + r_b \\ \dot{r}_b &= 0 \end{aligned} \tag{3}$$

In the equations, r_b represents the low frequency disturbance factor which models wind influence and the motion asymmetry caused by propeller rotation in a single propeller propulsion system, and r represents course changes caused by rudder action.

Corresponding linear models are:

- Nomoto's second-order model:

$$G_{\psi\delta}(s) = \frac{\psi(s)}{\delta(s)} = \frac{k}{s} \cdot \frac{(s+1/T_3)}{(s+1/T_1)(s+1/T_2)} = \frac{G_{r\delta}(s)}{s} \tag{4}$$

and

- Nomoto's first-order model:

$$G_{\psi\delta}(s) = \frac{\psi(s)}{\delta(s)} = \frac{k}{s(sT+1)} = \frac{G_{r\delta}(s)}{s} \tag{5}$$

The models are adequate to the real ship's behaviour for small rudder angles only and corresponding small values of yaw and sway velocities. Large rudder angles and course instability effects are better mapped by models with nonlinear terms. Thus, simple nonlinear models can be obtained:

- Bech's model based on Nomoto's second-order model:

$$\dddot{\psi} + \left(\frac{1}{T_1} + \frac{1}{T_2}\right)\ddot{\psi} + \frac{k}{T_1 T_2} H(\dot{\psi}) = \frac{k}{T_1 T_2}\left(\delta + T_3\dot{\delta}\right) \tag{6}$$

with

$$H(\dot{\psi}) = a_3\dot{\psi}^3 + a_2\dot{\psi}|\dot{\psi}| + a_1\dot{\psi} + a_o$$

- Norrbin's model based on Nomoto's first-order model:

$$T\ddot{\psi} + a_3\dot{\psi} + a_2\dot{\psi}|\dot{\psi}| + a_1\dot{\psi} + a_o = k\delta \tag{7}$$

and

- a nonlinear version of the model (3):

$$\begin{aligned} \dot{v} &= a_{11}v + a_{112}v|v| + a_{12}ur + b_1u^2\delta \\ \dot{r} &= a_{21}v + a_{212}v|v| + a_{22}r + a_{222}r|r| + b_2u^2\delta \\ \dot{\psi} &= r + r_b \\ \dot{r}_b &= 0 \end{aligned} \tag{8}$$

The (3) to (8) models were converted to the discrete form before their identification.

NEURAL MODEL

Artificial neural networks are formed from artificial neurons. The artificial neuron is a simple model of the biological one. Fig. 3 presents its structure. The input signals are multiplied by associated weights and added together. Output signal is computed by using the function of activation f.

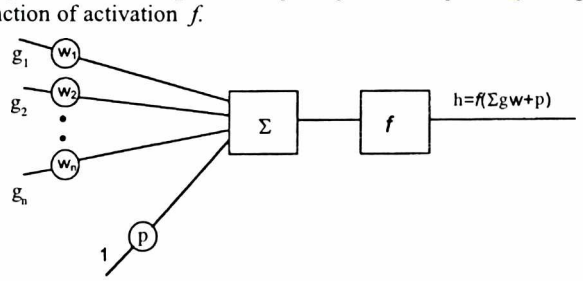

Fig. 3. The structure of the artificial neuron

A set of parallelly connected neurons is the layer. Two or three layers can form the network. Basic neural structures used for dynamic system identification are described in [4]

The neural model used for the ship motion model identification represented a serial-parallel structure. Both output and input signals of the physical model were fed to the neural model. The nonlinear dynamics of a discrete SISO model can be expressed as follows:

$$h_{k+1} = F\left[h_k, h_{k-1}, \ldots, h_{k-n+1}\ ;\ g_k, g_{k-1}, \ldots, g_{k-m+1}\right] \quad (9)$$

where $F[.]$ denotes a nonlinear function which describes mapping present and previous input and output values to a next step value of the output. In the neural model the unknown nonlinear function F is approximated by the neural network $N[.]$. Hence the neural interpretation of the ship dynamics can be expressed as follows:

$$\dot{\psi}_{k+1} = N\left[\dot{\psi}_k, \dot{\psi}_{k-1}, \ldots, \dot{\psi}_{k-n+1}; \delta_{k-1}, \delta_{k-2}, \ldots, \delta_{k-m+1}\right] \quad (10)$$

where:

k, m, n - time instants

The multilayered feedforward neural network can approximate any nonlinear mapping [2]. This feature allows for using a three layered feedforward network for the ship model dynamics identification. A sigmoidal function is applied as the activation function for the first two layers. The third layer output is linear.

MEASUREMENT SYSTEM, FILTRATION, AND PROCESS VARIABLES ESTIMATION

Fig. 4 presents the measurement system diagram. The dash-dot line separates the part installed on the ship model. The PC computer linked to the positioning system and VHF transmitter are placed on the lake bank. The ashore part of the system measures and computes x and y coordinate values in the X_0Y_0 local coordinate system, then sends them to the model through the radio modem. Transmission speed is set to 2 records per second.

The computer onboard the model records the following signals, apart from the coordinate values:

- the rudder angle (10 patterns/second)
- the course angle from the gyrocompass through a RS-422 interface (1200 baud)
- drives' setpoint values, and
- the model course received from the magnetic compass (10 patterns/second).

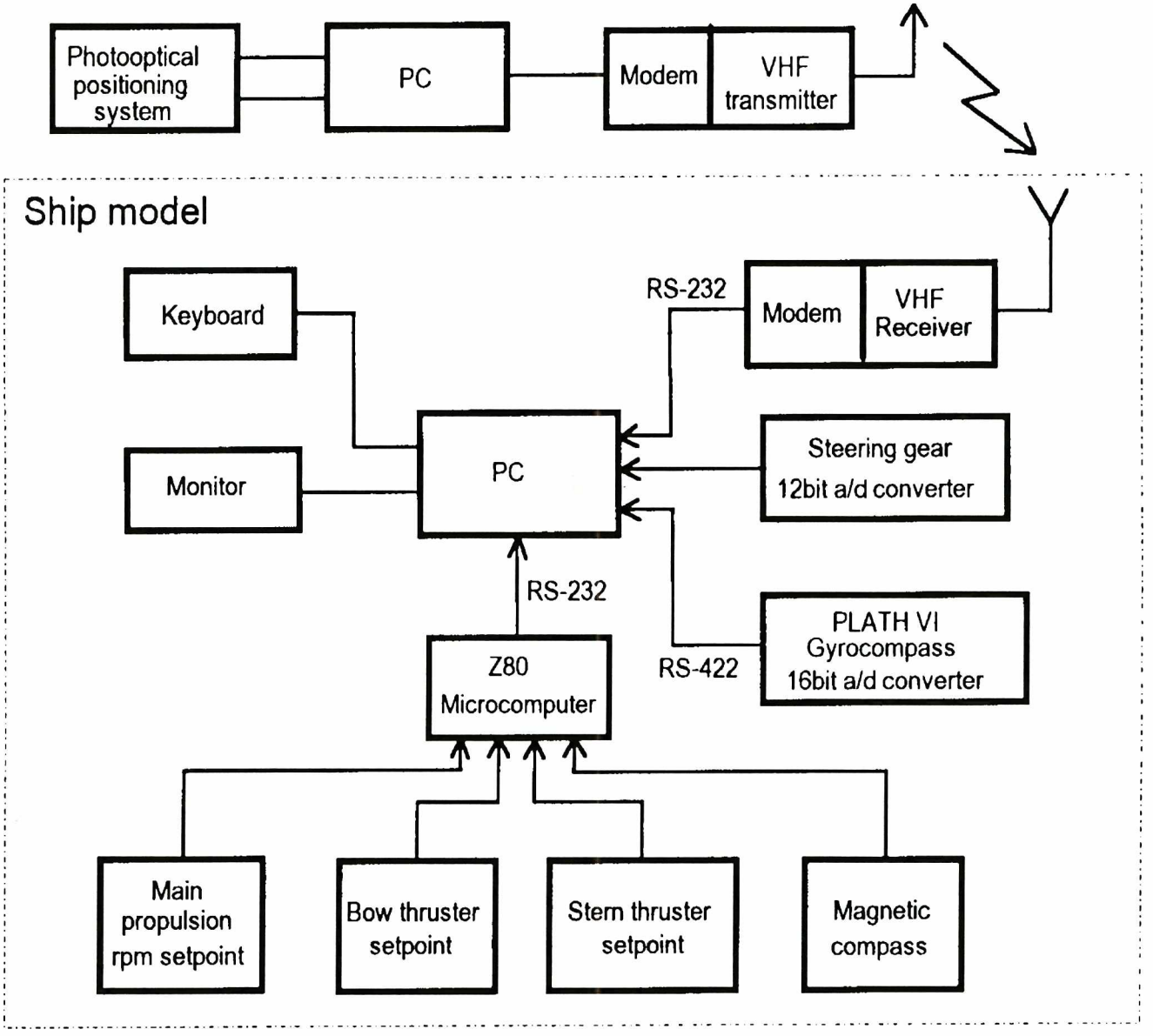

Fig. 4. Measurement system diagram

The recording cycle of the data is in compliance with a cycle of data transmission through the radio modem. Internal frequency of each device was not synchronized so every record, added to a file on a disk, acquired last signal values maintained in memory buffers. Data repetitions and losses are usual for the recording method. The faults can be caused by fadings in a radio channel and the erroneous data reading when a few values are received simultaneously from different simplex serial interfaces by using the same interruption (Q3, Q4). In the positioning system errors can be induced by infrared signal decays on the edge of the system range, an accidental infrared source covering and random sunlight or infrared light reflections on water surface. Hence the recorded values were verified and off-line preprocessed before being used for the mathematical model identification.

The following variables were used to identify the model employed in a course control process:

- x, y ship model coordinates
- ψ course angle
- δ rudder angle

Fig. 5 presents an example of „Warta" tanker model trajectory recorded during the experiment.

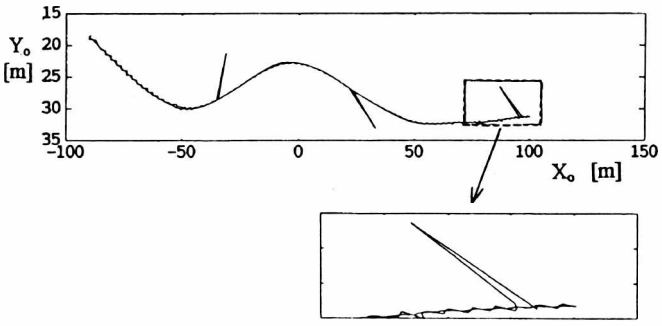

Fig. 5. An example of the recorded and filtered ship model trajectories

Longitudinal and transverse velocities of the model geometrical centre were determined by using the measured model coordinates and heading angle. The following equations were applied:

$$\hat{u}_k = \hat{\dot{x}}_k \cdot \sin(\hat{\psi}_k) + \hat{\dot{y}}_k \cdot \cos(\hat{\psi}_k)$$
$$\hat{v}_k = \hat{\dot{x}}_k \cdot \cos(\hat{\psi}_k) - \hat{\dot{y}}_k \cdot \sin(\hat{\psi}_k) \tag{11}$$

where symbol ^ denotes estimated values. Components of the $\dot{x}_k$ and $\dot{y}_k$ velocities were estimated by Kalman filtering. The filter is based on a digital model with a state vector which contains the coordinates and velocity components related to the earth-fixed coordinate system [2]:

$$\bar{x}_{k+1} = A \cdot \bar{x}_k + \bar{w}_k$$
$$\bar{x}_k^T = [\dot{x}_k, x_k, \dot{y}_k, y_k] \tag{12}$$

Measurement equation has a form:

$$\bar{z}_k = \mathrm{B} \cdot \bar{x}_k + \bar{v}_k$$
$$\bar{z}_k^T = [x_k, y_k] \tag{13}$$

where:

$$A = \begin{bmatrix} 1 & 0 & 0 & 0 \\ t_p & 1 & 0 & 0 \\ 0 & 0 & 1 & 0 \\ 0 & 0 & t_p & 1 \end{bmatrix}$$
$$B = \begin{bmatrix} 0 & 1 & 0 & 0 \\ 0 & 0 & 0 & 1 \end{bmatrix} \tag{14}$$

$\bar{v}_k$ - the measurement noise vector

$\bar{w}_k$ - the disturbance vector which describes the model motion randomness

T - the transposition symbol

Independent error characteristics of both photooptical sensors, mean values of measurement noises equal to zero and their variances equal to σ, were assumed. It means that:

$$\mathrm{E}[v_k] = 0 \tag{15}$$

and the measurement noise covariance matrix is [3]:

$$R_k = E[v_k, v_k^T] = \begin{bmatrix} c^2 \cdot K_{xx} \cdot \sigma_\alpha^2 & c^2 \cdot K_{xy} \cdot \sigma_\alpha^2 \\ c^2 \cdot K_{xy} \cdot \sigma_\alpha^2 & c^2 \cdot K_{xx} \cdot \sigma_\alpha^2 \end{bmatrix} \tag{16}$$

where:

K_{xx}, K_{yy}, K_{xy} - nonlinear functions of model position coordinates

c - distance between optical sensors

The best measurement accuracy was obtained when model position was contained within: $-0.5c<x<0.5c$ and $0<y<c$. The real value of the coordinates measurement variance depended on the distance from optical sensors and on atmospheric conditions; it was contained within $0.01 \div 0.064 \cdot 10^{-4}$ m^2.

The measured coordinates were verified before filtering. Impulse noises and fadings could cause large errors in the filter output. To eliminate impulse noises a heuristic method was applied. At each time point the measured coordinates were compared with one-step-ahead predictions of their values. When the measured value lay within a confidence rectangle, the measurement was accepted, otherwise, the measured value was replaced by its estimate. Dimensions of the confidence rectangle in the XY coordinate system were chosen as triple variance values counted from the equations:

$$\sigma_x = c \cdot K_{xx} \cdot \sigma_\alpha = c \cdot \sigma_\alpha \cdot \sqrt{\left(0.5 - \frac{x}{c}\right)^2 \cdot \left(\frac{c}{y}\right)^2 \cdot \left[\left(0.5 + \frac{x}{c}\right)^2 + \left(\frac{y}{c}\right)^2\right]^2 + \left(0.5 + \frac{x}{c}\right)^2 \cdot \left(\frac{c}{y}\right)^2 \cdot \left[\left(0.5 - \frac{x}{c}\right)^2 + \left(\frac{y}{c}\right)^2\right]^2}$$
$$\sigma_y = c \cdot K_{yy} \cdot \sigma_\alpha = c \cdot \sigma_\alpha \cdot \sqrt{\left[\left(\frac{y}{c}\right)^2 + \left(0.5 - \frac{x}{c}\right)^2\right]^2 + \left[\left(\frac{y}{c}\right)^2 + \left(0.5 + \frac{x}{c}\right)^2\right]^2} \tag{17}$$

where σ_α denotes the variance of the optical detector bearing angle. In the case of measurement fadings detected by the computer connected to the optical positioning system, the measured values were also substituted by their estimates. An example of the recorded and filtered model trajectories is shown in Fig 5.

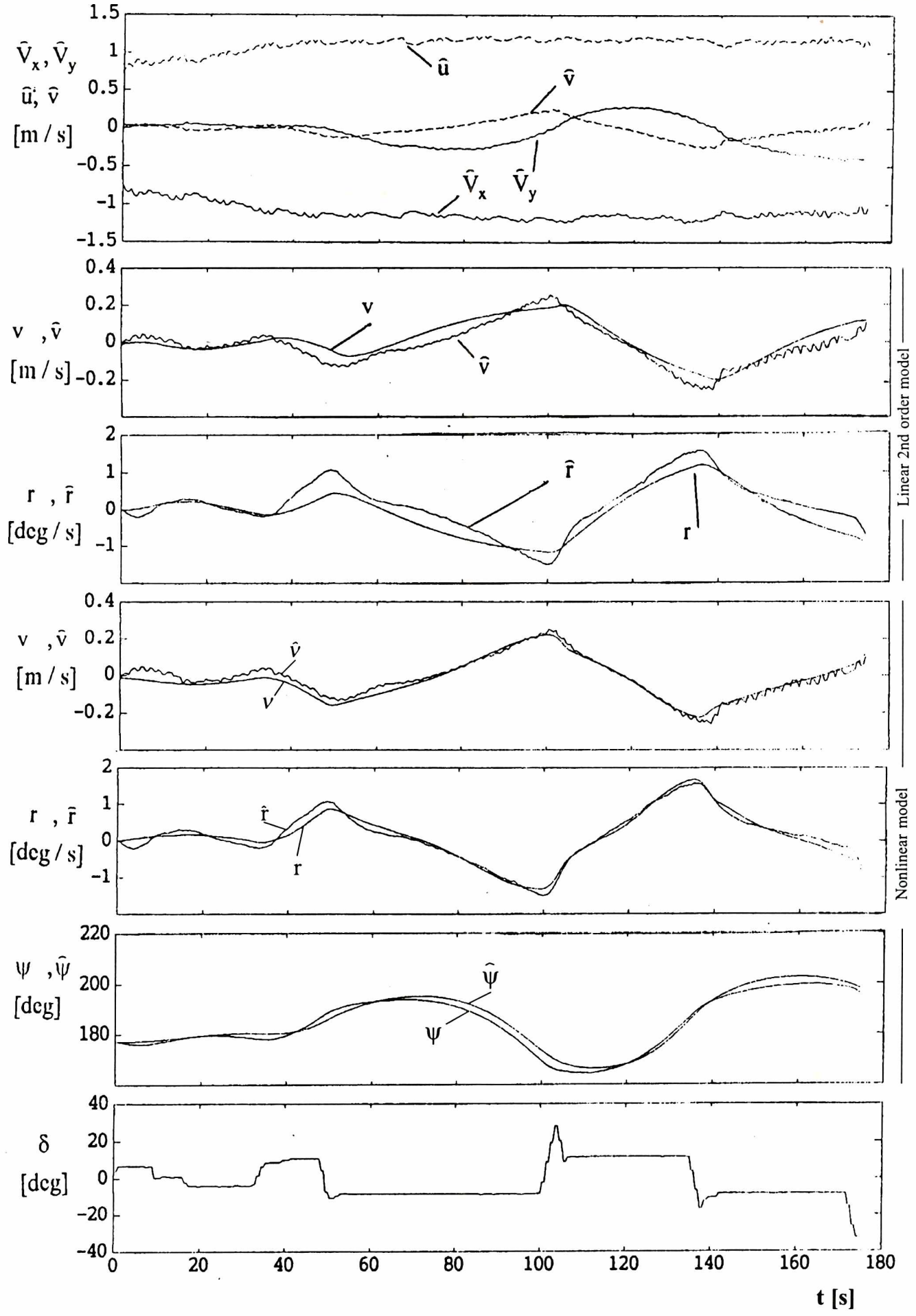

Fig. 6. Identification results of the model (3) and (8)

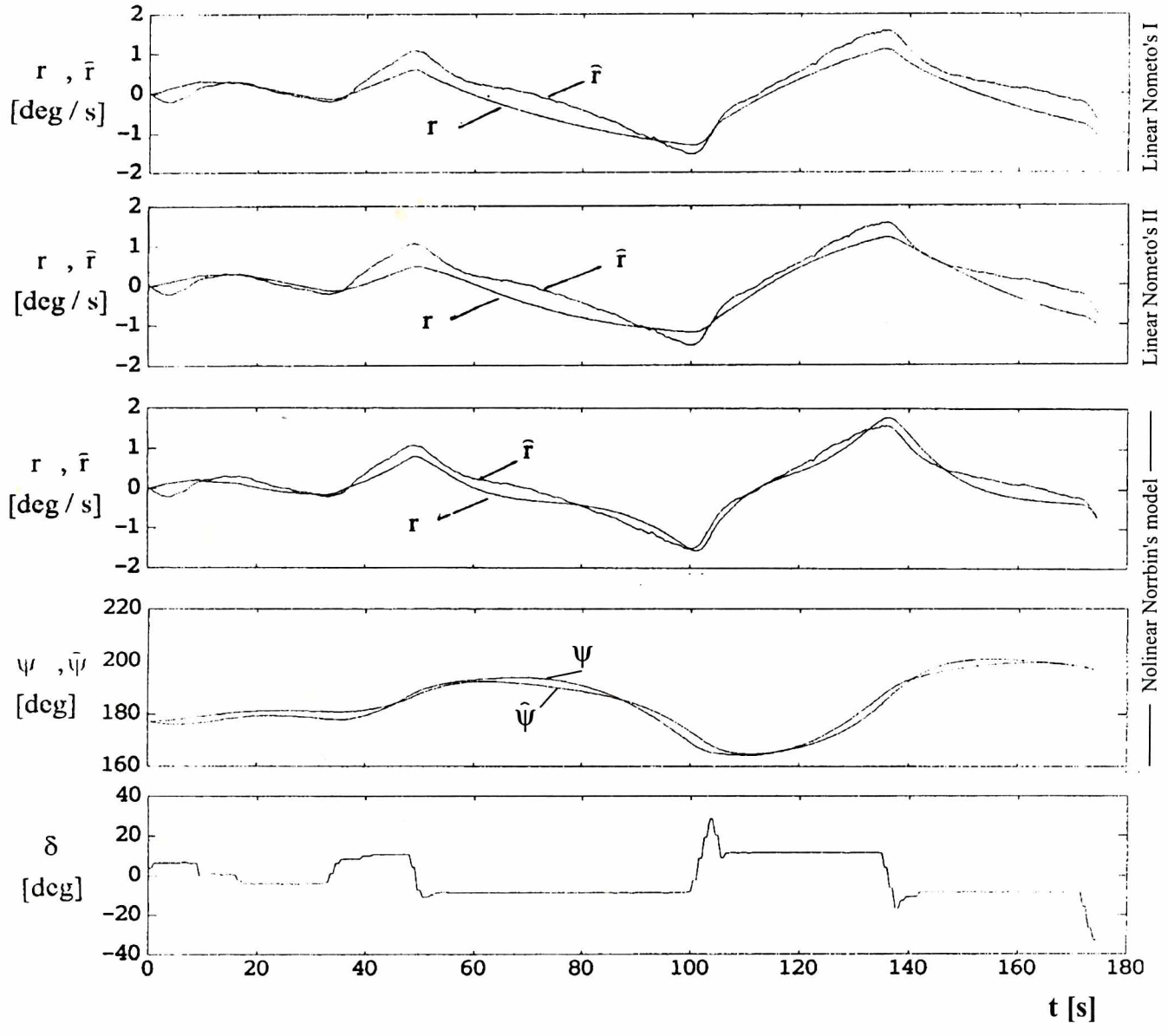

Fig. 7. Identification results of Nomoto's and Norrbin's models

EXPERIMENT RESULTS

The trajectories, heading angles and rudder angles of the ship model were measured at the different model velocities (dead slow - 0.41 m/s, slow - 0.71 m/s, half speed - 0.83 m/s, full speed - 1.13 m/s), different course changes and different rudder angles. MATLAB toolboxes were used to identify the mathematical models. Linear and nonlinear mathematical models were transformed to PEM (predictive error model) structure and identified in this form. Estimates of the model heading ψ, yawing velocity r and transverse speed v were used for the identification. The decomposition was applied to estimate mathematical model parameters in the first step, and the slow-varying component of the yawing velocity r_b caused by wind- and propeller-induced moments, in the second.

Fig. 6 and Fig. 7 present velocities and angle changes for the zig-zag test (interrupted) performed at full speed (the corresponding trajectory is presented in Fig. 5). Recorded values of the transverse velocity v, angular velocity r, and the rudder angle δ are compared in the figures with the values obtained from the identified mathematical models. Fig. 7 presents output values (angular velocity) of linear Nomoto's 1st- and 2nd-order models and one-dimensional nonlinear model of Norrbin. Fig. 6 shows the estimated velocities $\hat{V}_x$, $\hat{V}_y$ in the ground-fixed coordinate system X_oY_o, estimated values of longitudinal and transverse velocities of the physical model and the corresponding values from the identified linear and nonlinear mathematical models. The parameters of the (3) to (8) models are shown in Tab. 2 and 3.

Tab. 2. SISO model parameters

Model	k	T	T_1	T_2	T_3	a_1/T	a_2/T	a_3/T	k/T	r_b
Nomoto's I (5)	0.2218	36.3636	-	-	-	-	-	-	-	0.1685
Nomoto's II (4)	0.5893	-	10.6045	15.9236	3.4977	-	-	-	-	0.0122
Norrbin's (7)	-	-	-	-	-	-0.1530	0.1153	0	0.0069	0.0773

Tab. 3. MIMO model parameters

Model	a_{11}	a_{12}	a_{21}	a_{22}	$b_1\times10^{-2}$	$b_2\times10^{-2}$	a_{112}	a_{212}	a_{222}	r_b
Linear (3)	-0.3733	-0.0631	1.1981	0.1828	0.3903	0.1881	-	-	-	0.1677
Nonlinear (8)	-0.1747	-0.0071	-0.2580	0.1628	-0.0598	0.3728	-0.2930	4.6563	0.0506	-0.0106

The identification of the two-dimensional linear model (3) was performed too. Standard turning circle tests were applied to the tanker model. Fig. 8 shows the trajectories of the model going full-ahead (app. 0.9 m/s). The form of the trajectories indicates asymmetrical behaviour of the model caused by its single propeller propulsion system.

Like in other tests, the measured position coordinates were used to estimate the transverse and angular velocities of the ship model. The velocities together with the rudder angle signal were

utilized to identify the model (3). The parameters of the model were computed on the basis of the corresponding discrete ARX and PEM models. Examples of the estimated and identified values of the transverse and angular velocities are shown in Fig. 9. Parameters of the linear model (3) identified by using the ARX and PEM models are presented in Tab.4 and 5.

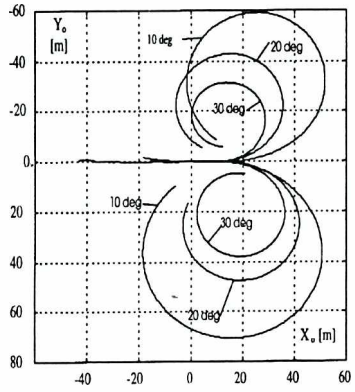

Fig. 8. „Warta" model trajectories during the turning circle trials (V=1.3 m/s, δ=±10 =10 deg, ±20 deg, ±30 deg)

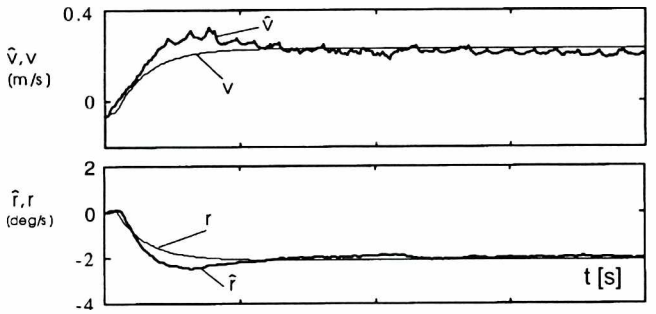

Fig. 9. The measured and identified (ARX model) values of the transverse v and angular r velocities of „Warta" model (V = 1.3 m/s, δ = -20 deg).

The network used in the identification process of the SISO model belonged to the class $\Gamma_{5,10,1}$. It means that the network consisted of 5 neurons in the first layer, 10 neurons in the second and 1 neuron in the third. This type of the neural model structure can be easily converted into a multidimensional case. The presented results show the outcome of the MIMO neural model obtained by adding transverse and longitudinal velocities to the SISO model (10). In this case the network belonged to the class $\Gamma_{10,10,3}$.

Tab.4. The parameters of the two-dimensional linear model (3) calculated from identification of the ARX model in standard turning circle tests at the velocity V≈1.3 m/s

δ [deg]	a_{11}	a_{12}	a_{21}	a_{22}	b_1	b_2	r_b
-30	-0.27141	-0.02004	0.403819	-0.072157	-0.00073	0.00849	-0.06698
-20	-0.12483	-0.01096	-0.19256	-0.107939	-0.00054	0.00835	-0.03412
-10	-0.31213	-0.04061	0.25670	-0.002791	-0.00074	0.00674	-0.06244
10	-0.27435	-0.03697	-0.12991	-0.084448	-0.00030	0.008682	0.023914
20	-0.28261	-0.03172	0.311675	-0.054936	-0.00040	0.00807	0.003009
30	-0.20471	-0.02186	0.078969	-0.081686	-0.00015	0.00579	0.072389

Tab. 5. The parameters of the two-dimensional linear model (3) calculated from identification of PEM model in standard turning circle tests at the half-ahead velocity V ≈ 0.93 m/s

δ [deg]	a_{11}	a_{12}	a_{21}	a_{22}	b_1	b_2	r_b
-30	-0.45479	-0.0396	0.77376	-0.057254	-0.00075	0.009997	-0.06698
-20	0.07920	0.02418	-1.05696	-0.249964	-0.00134	0.010947	-0.03412
-10	-0.38631	-0.05183	0.709999	0.046188	-0.00064	0.009021	-0.06244
10	0.029028	0.015267	-1.279591	-0.225983	-0.00143	0.005829	0.023914
20	-0.36642	-0.05006	2.028283	0.244235	0.000254	0.001284	0.003009
30	-0.17249	-0.01937	0.93359	0.041719	0.000019	0.003915	0.072389

Fig. 10 presents identification results of both models. An altered data set was used for identification of the MIMO model. The model generated large impulse disturbances when the rudder angle had been changed rapidly. High frequency noises were observed in outputs of both neural models. The disturbances are included in the input data hence more filtration is necessary before the neural identification.

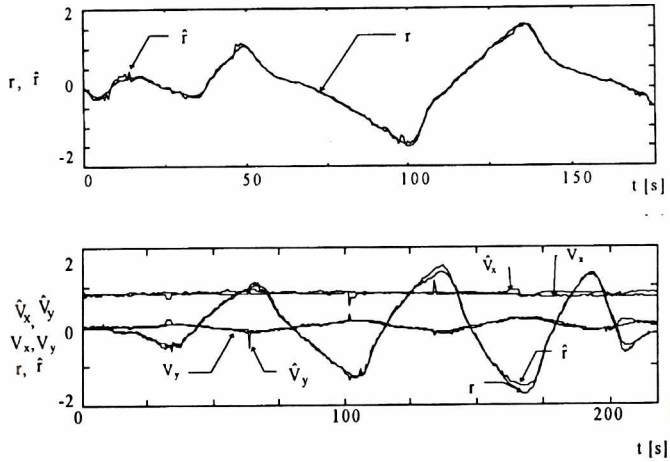

Fig. 10. Identification results of the neural models

CONCLUSIONS, SUMMARY OF EXPERIENCE

The presented results of experiments show that the identification methods applied to the physical ship model are suitable and can be also used to full scale vessels. However ship's position must be measured with proper accuracy. The precise position data are necessary to estimate ship transverse velocity. A dual-axis log is insufficient to measure this velocity due to large log errors involved during rapid course changes.

The experiments revealed that nonlinear mathematical models fitted better to the physical model than linear one, even if the rudder angle did not reach ±35°. The manoeuvres were limited by a confined water area, many navigation obstacles and range of the positioning system. The tests did not confirm linear or quadratic relationships between the identified mathematical model parameters and the physical model velocity. For nonlinear models a considerable convergence of physical and mathematical model responses was observed. The mathematical model parameters yield Dieudonné's curve unnatural for full scale vessels.

The turning circle tests indicated that the linear model complied with the physical one when the longitudinal velocity had been stable and the angular and transverse velocities changeable. When the heading angle changes had been large the longitudinal velocity decreased and caused overshoot effect of the angular and longitudinal velocities. Thus, the identified second-order linear model obviously has complex eigenvalues.

This effect is confirmed by the identification results of the model (3) based on the PEM model.

A high mapping accuracy was observed in the case of the neural identification. The precision is significant particularly when comparing the SISO neural and classical models. An advantageous aspect of the neural models is the weak relationship between the mathematical model performance and the ship model velocity variation. The neural model tested for one set of data very well approximated ship's behaviour for another set of data. A significant disadvantage of the neural identification is long learning process. More than 15 000 learning epochs were repeated to learn the SISO model and more than 50 000 to learn the three-dimensional model.

Acknowledgement

This work was financially supported by State Committee for Scientific Research (Grant PB 878/T11/95/08).

NOMENCLATURE
(except of symbols directly highlighted in the text)

a_i - nonlinear model coefficients
a_{ijk} - nonlinear model coefficients
a_{ij} - state matrix coefficients
b_i - steering matrix coefficients
E - variance
F - nonlinear function
g_i - neuron input signals
$G_{r\delta}$ - rudder angle-angular speed transmittance
$G_{y\delta}$ - rudder angle-course angle transmittance
h_i - neuron output signals
k - transmittance amplification factor
N - nonlinear function mapped by neuron network
p - permanent displacement
r - ship yawing velocity ($r = d\psi / dt = \dot{\psi}$)
r_h - low frequency disturbance factor (component of r)
s - Laplacian
t - time
t_p - sampling period
T, T_i - time constants
u_0 - stillwater steady speed
v - sway velocity
V - ship velocity
V_x, V_y - components of V in $X_0 Y_0$ reference system
w_i - neuron weighting coefficients
x,y,z - ship coordinates in $X_0 Y_0 Z_0$ reference system
X, Y, Z - hull-fixed Cartesian reference system
$X_0 Y_0 Z_0$ - earth-fixed Cartesian reference system
δ - rudder angle
$\sigma_x, \sigma_y, \sigma_a$ - variances of : x, y coordinates and sensor bearing angle, respectively
ψ - ship heading (course angle)
$\wedge, \cap$ used as upper indices denote estimated values

BIBLIOGRAPHY

1. Abkowitz, M. A.: „Lectures on Ship Hydrodynamics - Steering and Manoeuvrability". Technical Report Hy-5. Hydro- and Aerodynamic's Laboratory. Lyngby, 1964
2. Hertz J., Krogh A., Palmer R.G.:„ Introduction to the Theory of Neural Computation". Addison-Wesley Publ. 1991
3. Holejko K., Siuzdak J.: „Optoelectronic System for the Measurement of Ship Models Trajectory". IEEE Journal of Oceanic Engineering, 1991, vol. 16, no 4
4. Narendra K. S., Parthasarathy K.:„ Identification and Control of Dynamical Systems Using Neural Networks". IEEE Tans. Neural Networks, 1990, vol. 1, no 1
5. Norrbin N. H.: „ On the Added Resistance Due to Steering on a Straight Course". International Towing Tank Conference. Berlin, 1974
6. PC-Matlab Version 4.0: „ User's Guide ". The MathWorks Inc., 1992

Appraised by Józef Lisowski, Prof., D.Sc., E.E.

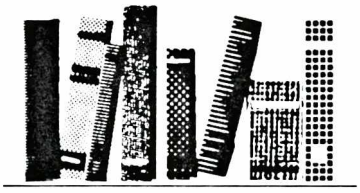

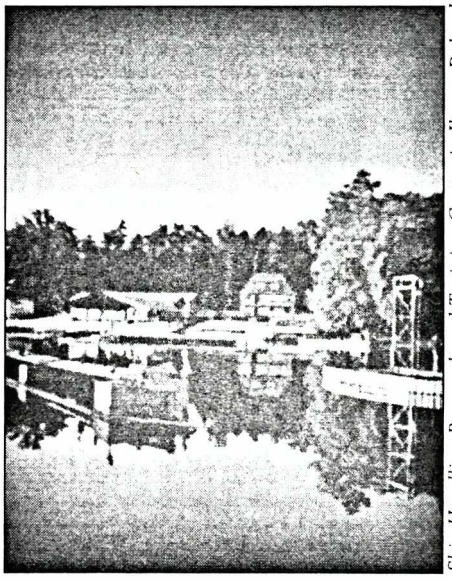

Ship Handling Research and Training Centre in Hawa, Poland

Current reports

TECHNICAL UNIVERSITY OF SZCZECIN
FACULTY OF MARITIME TECHNOLOGY
OCEAN AND SHIP TECHNOLOGY INSTITUTE

Automatic gas leakage detection in the condenser water space of refrigeration facilities

Freons frequently applied in the refrigeration facilities are highly penetrating gases, and the water space of condensers used in the facilities is especially exposed to leakages. In result, it quite often happens that the refrigerant penetrates into the condenser water space, and a lack of it in the installation causes the defective, and thus inefficient, operation of the refrigeration facility. Freon loss should be automatically indicated without condenser stopping, as the condenser water space is not accessible while operating.

The device, which makes doing if possible, has been designed in the Refrigeration Department, Technical University of Szczecin.

The thus far applied methods of leakage detection in the condenser water space consist in detecting gas bubbles in the water discharged out of the condenser. Such methods do not however provide any unique results, moreover the cost of the applied gauges is rather high. In the novel device made by Technical University of Szczecin common, much cheaper gauges for the detecting of the chemical compounds containing halogen molecules are used. The gauges have to work in a gas environment to operate suitably.

The gauge detector is separated from the condenser water space by means of a gas-only-penetrable membrane. The gauge is fitted in such a location as to ease the gas, which leaks through a point of untightness, being lighter than water, to penetrate into the lower part of the gauge and then through the membrane to the detector, thus starting its work.

Bogusław Zakrzewski, D. Sc., is the author of the device.